Cell Tissue Res (1993) 274:405–412

Cell & Tissue Research

Ferritin accumulation and uroporphyrin crystal formation in hepatocytes of C57BL/10 mice: a time-course study

Peter D. Siersema[1], **Maud I. Cleton-Soeteman**[2], **Wim C. de Bruijn**[3], **Fiebo J.W. ten Kate**[4], **Henk G. van Eijk**[2], **J.H. Paul Wilson**[1]

[1] Department of Internal Medicine, University Hospital Rotterdam-Dijkzigt, Dr. Molewaterplein 40, NL-3015 GD Rotterdam, The Netherlands
[2] Department of a Chemical Pathology, Erasmus University Rotterdam, NL-3015 GE Rotterdam, The Netherlands
[3] Department of Pathology, Erasmus University Rotterdam, NL-3015 GE Rotterdam, The Netherlands
[4] Department of Pathology, Academical Medical Centre, NL-1105 AZ Amsterdam, The Netherlands

Received: 1 February 1993 / Accepted: 26 March 1993

Abstract. To establish the time-sequence relationship between ferritin accumulation and uroporphyrin crystal formation in livers of C57BL/10 mice, a biochemical, morphological and morphometrical study was performed. Uroporphyria was induced by the intraperitoneal administration of hexachlorobenzene plus iron dextran and of iron dextran alone. Uroporphyrin crystal formation started in hepatocytes of mice treated with hexachlorobenzene plus iron dextran at 2 weeks and in mice treated with iron dextran alone at 9 weeks. In the course of time, uroporphyrin crystals gradually increased in size. Uroporphyrin crystals were initially formed in hepatocytes in the periportal areas of the liver, in which also ferric iron staining was first detected. The amount and the distribution of the main storage form of iron in hepatocytes, ferritin, did not differ between the two treatment groups. Ferritin accumulation preceded the formation of uroporphyrin crystals in hepatocytes in both treatment groups. Moreover, uroporphyrin crystals were nearly always found close to ferritin iron. We conclude that uroporphyrin crystals are only formed in hepatocytes in which also iron (ferritin) accumulates. Hexachlorobenzene accelerates the effects of iron in porphyrin metabolism, but does not influence the accumulation of iron into the liver.

Key words: Liver – Hepatocytes – Ferritin – Iron – Uroporphyrin – Uroporphyria – Hexachlorobenzene – Mouse

Introduction

Both human and experimental uroporphyria are characterized by a partial block in the haem biosynthetic pathway at the level of uroporphyrinogen decarboxylase (URO-D; EC 4.1.1.37) and by the accumulation of uroporphyrins and heptacarboxylporphyrins in the liver (Sweeney 1986). In C57BL/10 mice, uroporphyria can be induced by the administration of hexachlorobenzene (HCB), a polyhalogenated aromatic hydrocarbon (Marks 1985), and iron dextran as Imferon (IMF), but also by the administration of IMF alone (Smith and De Matteis 1990; Siersema et al. 1991).

There is considerable evidence implicating iron in the pathogenesis of human and experimental uroporphyria (Sweeney et al. 1979; Smith and Francis 1983; Ferioli et al. 1984; Alleman et al. 1985; De Matteis 1988; Siersema et al. 1991). In the experimental form, the action of iron may involve the catalysis of the highly reactive hydroxyl radical (OH·) (Aust and Svingen 1982; Halliwel and Gutteridge 1985) or perhaps the production of reactive iron-oxygen species (Samokyszyn et al. 1988), which could react with uroporphyrinogen or another susceptible target to form an inhibitor of URO-D (Rios de Molina et al. 1980; Cantoni et al. 1984; Smith and Francis 1987). Alternatively, damage to URO-D either by a direct action of iron or by a free radical-mediated mechanism has been postulated (Mukerji et al. 1984).

Recently, we observed in hepatocytes of porphyric mice a morphological co-occurrence of uroporphyrin crystals and iron (ferritin) and suggested a role for ferritin iron in the pathogenesis of uroporphyria (Siersema et al. 1991). This study was conducted at 18 weeks after treatment with HCB plus IMF and with IMF alone. At this time diffuse iron (as ferritin) and focal uroporphyrin accumulation already existed. Therefore, we decided to perform biochemical, morphological (light microscopical [LM], electron microscopical [EM]) and morphometrical studies in livers of C57BL/10 mice. We aimed to establish the time-sequence relationship between uroporphyrin crystal formation and ferritin iron accumulation at regular intervals from 1 week until 52 weeks, after the intraperitoneal administration of HCB plus IMF and of IMF alone.

Correspondence to: P.D. Siersema

Materials and methods

Chemicals

HCB was purchased from Merck AG (Darmstadt, Germany), ferrihydroxide-dextran complex in a 0.9% NaCl solution (Imferon) was purchased from Fisons Pharmaceuticals (Vleusden, The Netherlands) and Avertin from Aldrich-Chemie GmBH & Co. (Steinheim, Germany). All other chemicals were of the highest purity commercially available.

Animals and treatment

This study was performed according to the "Regulations for use of laboratory animals in the Erasmus University Rotterdam", laid down by the Laboratory Animal Committee of the Erasmus University Rotterdam, The Netherlands.

Male C57BL/10 mice, weighing 20 to 25 gm, were purchased from the Centraal Proefdier Bedrijf (Zeist, The Netherlands). The mice were divided into three groups: group 1 and 2 consisted each of 45 mice, and group 3 consisted of 9 mice. Mice in group 1 were treated with 16 mg of HCB in two doses of 8 mg, on day 1 and day 4. HCB was dissolved in 0.25 ml warm corn oil and injected intraperitoneally (i.p.). Mice in groups 1 and 2 were treated with IMF, 12 mg per mouse, also injected i.p. on day 1. Treatment was performed under anaesthesia with Avertin. Mice in group 3 were not treated. At weekly intervals until week 15 and thereafter at weeks 20, 25, 30, 40 and 52, two mice of groups 1 and 2 were sacrificed for the morphological studies. In addition, at weeks 10, 20, 30, 40 and 52 the biochemical measurements were performed in livers of 3 mice in groups 1 and 2. Three mice from group 3 were sacrificed at weeks 0, 20 and 52 as controls for the morphological studies and the same biochemical measurements.

Under anaesthesia with Avertin, two liver lobes from the mice were removed for the measurement of the total porphyrin content and the total iron content. For the morphological studies, the portal vein was cannulated, and the liver was perfused with 3% glutaraldehyde in 0.14 mol/l cacodylate buffer, pH = 7.4 (275 mOsm). A perfusion rate of 10 ml/min, a perfusion pressure of 15 cm Hg, and a perfusion temperature of 37° C were maintained throughout the procedure.

Measurement of porphyrins

For the measurement of porphyrins in livers, the lobes were homogenized to yield a 10% homogenate in TRIS-HCl buffer (50 mmol/l, pH = 8.0), which was centrifuged for 10 min at 1800 *g*. After freeze-drying and methylation the porphyrins in liver tissue were measured by high pressure liquid chromatography as described earlier (Wilson et al. 1978; Siersema et al. 1991). Protein was measured according to Lowry et al. (1951). The amount of porphyrins was expressed in picomoles per milligram of protein.

Total iron content

This was determined using a modification of the method described by Harris (1978), which has been described previously (Siersema et al. 1991). The amount of iron was expressed as mmol/100 gm dry weight.

LM and EM studies

For LM, a part of the perfused liver was dehydrated briefly through graded alcohol series, embedded in paraffin, serially sectioned and stained. The staining protocol included Gill's hematoxylin stain (with reduced water contact) (James et al. 1980), the ferric ferricyanide reduction test in Lillie's modification (Lillie and Fullmer 1976), and Perls' Prussian-blue stain for ferric iron (Scheuer et al. 1962). For histological studies a Zeiss Axioplan microscope (Zeiss, Oberkochen, Germany) was used.

For EM, small blocks were taken randomly from the perfused livers, dehydrated briefly through graded acetone series and embedded in Epon (Siersema et al. 1991). Ultrathin sections (60 nm) were collected on copper grids and examined with and without conventional staining (uranyl acetate and lead citrate) in a Zeiss EM 902 transmission microscope (Zeiss, Oberkochen, Germany). This instrument is equipped with an integrated electron spectrometer allowing high-resolution imaging with energy-filtered electrons [= electron spectroscopic imaging (ESI)]. For technical details, see Sorber et al. (1990a, b).

Morphometrical analysis

This was performed as described in a previous report (Siersema et al. 1991). In brief, unstained Epon sections, 500- to 750 nm thick, were visualized by way of reflection-contrast microscopy, with the use of a Zeiss antiflex planneofluar, 63 × /1.25, Ph3, oil-immersion objective (Fig. 1) (Ploem 1975; Cornelese-ten Velde and Prins 1990). Images were transferred to the image analyser IBAS 2000 (Kontron/Zeiss, Munich, Germany) with a sensitive camera mounted on the Zeiss Axioplan microscope (Zeiss, Oberkochen, Germany). In sections of liver from each treatment group at the given time periods, 40 hepatocyte cytoplasmic areas of 8100 μm^2 were randomly selected. The area fractions (expressed as percentages of the measured cytoplasmic frame area) of uroporphyrin crystals and ferritin particles present in each area were calculated. Grey-value frequency histograms were used for objective segmentation and discrimination between ferritin and uroporphyrin crystals. For technical details, see Cleton et al. (1989) and Sorber et al. (1990a, b).

Statistics

Biochemical and morphometrical parameters in livers of the various groups at the different time intervals were tested for significant differences using the Wilcoxon's rank-sum test. The null hypothesis was rejected when $p \geq 0.05$.

Results

Biochemistry

Results of mean (±S.D.) porphyrin content and mean (±S.D.) iron content in livers in the control group of mice and in mice treated with HCB plus IMF and IMF alone at different times are given in Table 1. As can be seen from this table, up to week 30, porphyrin content in mice treated with HCB plus IMF was significantly more increased as compared with mice treated with MF alone. Thereafter, no significant difference in the increase in porphyrin content was observed between the two treatment groups. Throughout the whole study period, iron content was not different between mice treated with HCB plus IMF and mice treated with IMF alone.

Light microscopy

The lobular architecture of the livers from mice treated with HCB plus IMF and IMF alone remained intact

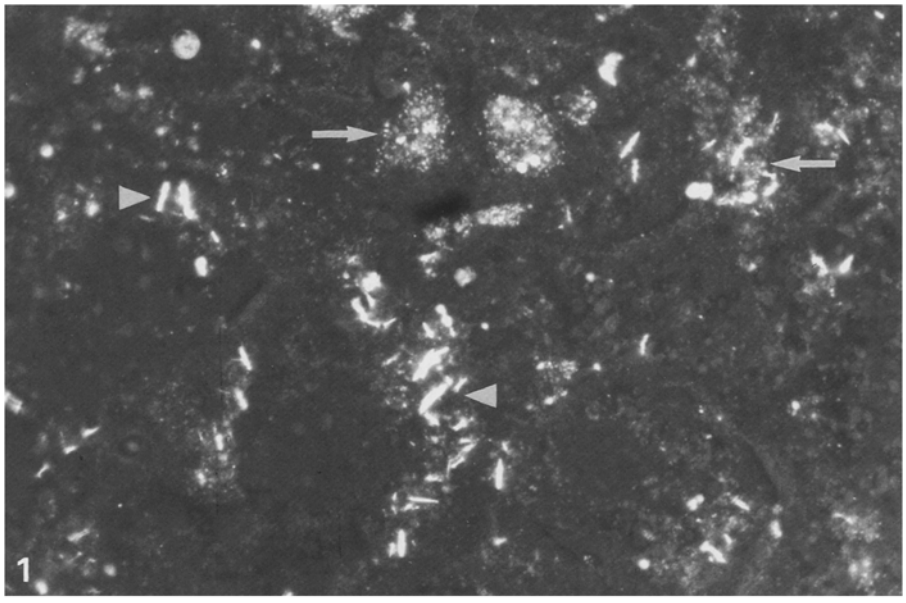

Fig. 1. Reflection-contrast micrograph of an unstained Epon section of mouse liver tissue, 20 weeks after treatment with iron dextran, showing uroporphyrin crystals (*arrowheads*) and ferritin particles (*arrows*). × 500

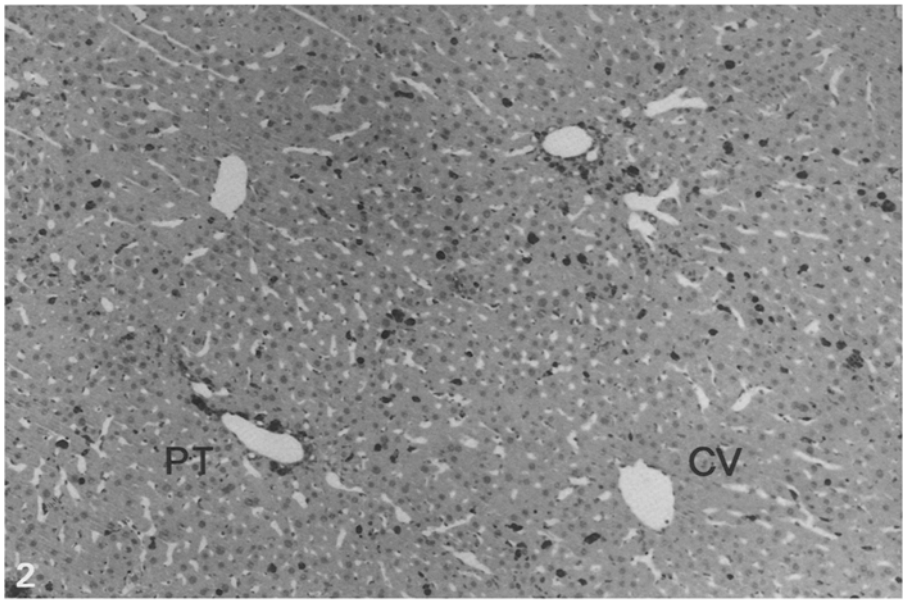

Fig. 2. Light micrograph, Perls' Prussian-blue stain of mouse liver tissue, 2 weeks after treatment with hexachlorobenzene and iron dextran. Note staining (indicating ferric iron) in the (peri)portal and midzonal areas of the liver. *PT* Portal tract; *CV* central vein. × 25

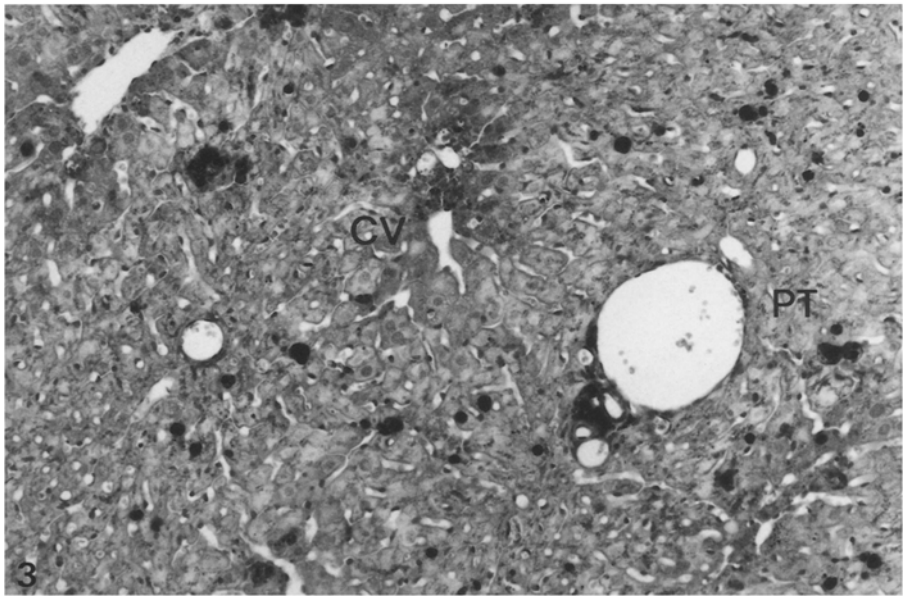

Fig. 3. Light micrograph, Perls' Prussian-blue stain of mouse liver tissue, 5 weeks after treatment with hexachlorobenzene and iron dextran. Note staining (indicating ferric iron) in the (peri)portal and the centrilobular areas of the liver. *PT* Portal tract; *CV* central vein. × 50

Table 1. Biochemical data of liver tissue in control mice and in mice treated with HCB and IMF, and with IMF alone. HCB, hexachlorobenzene; IMF, iron dextran; n.d., not done

Parameter	Duration of study (weeks)	Controls	Treatment groups	
			HCB+IMF	IMF
Porphyrin content[a]	0	2.0±0.5	n.d.	n.d.
	10	n.d.	198±31[c]	60±11
	20	1.8±0.4	391±62[c]	212±42
	30	n.d.	498±65[c]	345±68
	40	n.d.	543±101[d]	459±98
	52	2.1±0.5	569±122[d]	524±112
Iron content[b]	0	0.3±0.2	n.d.	n.d.
	10	n.d.	4.9±0.6[d]	4.7±0.7
	20	0.4±0.2	11.2±0.9[d]	11.6±1.1
	30	n.d.	12.9±1.2[d]	13.3±1.4
	40	n.d.	10.5±1.1[d]	9.9±1.3
	52	0.4±0.2	9.2±1.0[d]	9.4±1.2

[a] mean (±S.D.) in pmol per mg protein;
[b] mean (±S.D.) in mmol/100 gm dry weight;
[c] $P<0.05$ compared with IMF group;
[d] HCB+IMF group not different from IMF group

during the experimental period, i.e., the portal tracts did not show evidence of inflammatory infiltration or fibrosis. In addition, there was no liver cell necrosis in the lobular areas of the liver. At 3 weeks, the nuclei of the hepatocytes in both treatment groups appeared somewhat enlarged and some nuclei contained up to three nucleoli as compared with mice that were not treated. This was more pronounced in mice treated with HCB plus IMF than in mice treated with IMF alone. Concerning the aim of this study we did not further quantify this difference. In livers of mice treated with HCB, there was a patchy distribution of lipid droplets in the hepatocytes. This later finding can be attributed to the fact that HCB was dissolved in corn oil (Siersema et al. 1991).

During the whole period of the study, the pattern of iron deposition was not different between livers of mice treated with HCB plus IMF and with IMF alone. Immediately after the administration of IMF, iron-positive granules were observed in Kupffer cells. Thereafter, the amount of iron-positive granules in Kupffer cells increased and many of these cells became enlarged. Moreover, aggregates of iron-loaded macrophages ("siderophages") were formed. Initially, iron-loaded Kupffer cells were distributed diffusely throughout the liver lobules. By the 2nd week, iron-loaded Kupffer cells were observed to accumulate in the portal and periportal areas, but also spreading to the midzonal areas of the liver lobule (Fig. 2). By the 5th week, both Kupffer cells and siderophages, occurring singly or in small groups, were also noted in the centrilobular areas of the liver (Fig. 3). By the 2nd week, iron-positive granules were noted in hepatocytes, initially located close to the portal areas, but soon spreading to the midzonal areas of the

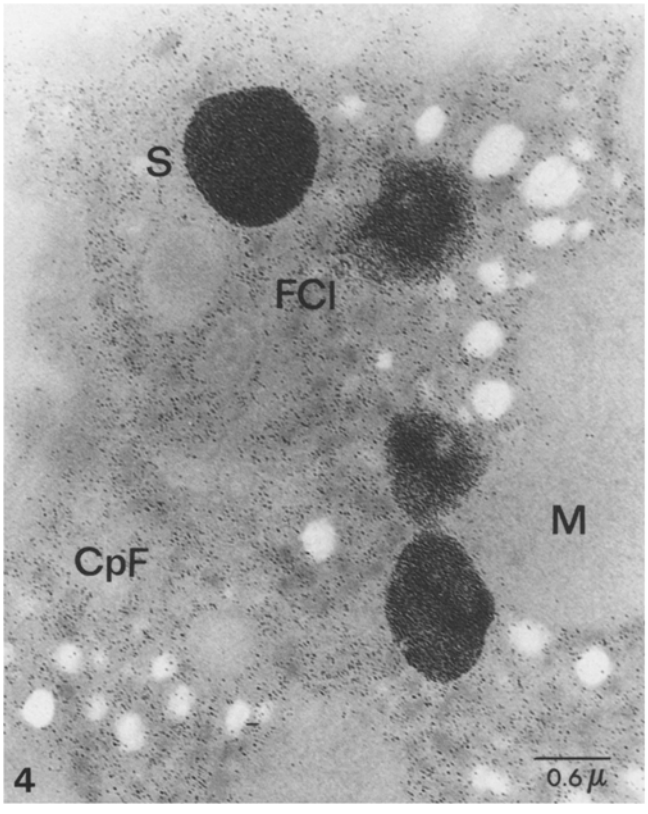

Fig. 4. Electron micrograph of a mouse hepatic parenchymal cell, 6 weeks after treatment with iron dextran. *S* Siderosome (iron-containing lysosome); *FCI* ferritin cluster; *CpF* cytoplasmic ferritin; *M* mitochondrion. Electron-spectroscopic image (ESI) of unstained section. *Bar*: 0.6 μm

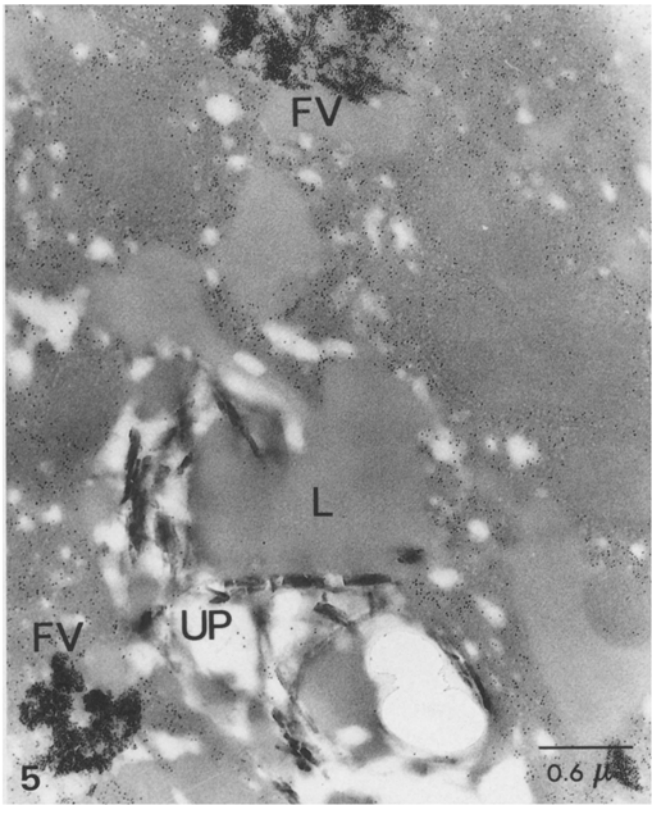

Fig. 5. Electron micrograph of a mouse hepatic parenchymal cell, 6 weeks after treatment with hexachlorobenzene plus iron dextran. *UP* Uroporphyrin crystal; *FV* ferritin-containing vacuole; *L* lipid droplet. Electron-spectroscopic image (ESI) of unstained section. *Bar*: 0.6 μm

liver lobule (Fig. 2). In the course of time, iron-positive staining in hepatocytes extended diffusely through the liver towards the centrilobular areas of the liver (Fig. 3). By week 6, siderosis of the liver was graded as massive [grade 4 according to Scheuer et al. (1962)]. After 52 weeks, Kupffer cells and siderophages, but also hepatocytes in the liver lobule still displayed a positive iron reaction. At this time, the highest concentration of iron-positive granules seemed to be present in the periportal areas.

Uroporphyrin crystals were first noted in hepatocytes of mice treated with HCB plus IMF by the 2nd week. The first uroporphyrin crystals were observed in those hepatocytes in which the first iron deposits were also detected, i.e., in the periportal areas of the liver (Fig. 1). The first uroporphyrin crystals were observed in hepatocytes of mice treated with IMF alone at the 9th week. During the entire study period, however, in both treatment groups uroporphyrin crystals were not regularly distributed but were usually found in those hepatocytes, in which also the highest concentrations of iron-positive granules were present, i.e., in the periportal areas and later also, although to a lesser degree, in the centrilobular areas of the liver.

Electron microscopy

Iron overload in hepatocytes of both treatment groups was initially seen as an increase and clustering of cytoplasmic ferritin. In addition, from 2 weeks onwards, ferritin was also found in siderosomes (iron-containing lysosomes) in hepatocytes (Fig. 4). At 6 weeks, the cellular organelles showed the characteristic signs of iron overload: indented heterochromatic nuclei, swollen endoplasmic reticulum, widened intercellular spaces sometimes containing collagen fibers, and flattened microvilli in the bile canalicular region. Apart from an increased amount of lipid droplets in hepatocytes of mice treated with HCB (which was dissolved in corn oil), no difference was observed in the ultrastructure between mice treated with HCB plus IMF and with IMF alone during the experimental period. Moreover, there was no difference in the pattern of distribution and in the storage forms of iron between hepatocytes of mice treated with HCB plus IMF and with IMF alone.

Uroporphyrin crystals in hepatocytes could be examined best in unstained Epon sections. Uroporphyrin crystals were randomly located in hepatocytes close to ferritin (Figs. 5, 6). Throughout the study period, it appeared that uroporphyrin crystals gradually increased in size (Figs. 5, 6).

Morphometrical analysis

The results of the morphometrical analysis in hepatocytes of mice treated with HCB plus IMF and with IMF alone are shown in Figs. 7, 8. As can be seen from these figures, the area fractions of ferritin in hepatocytes at the various time intervals were not different between

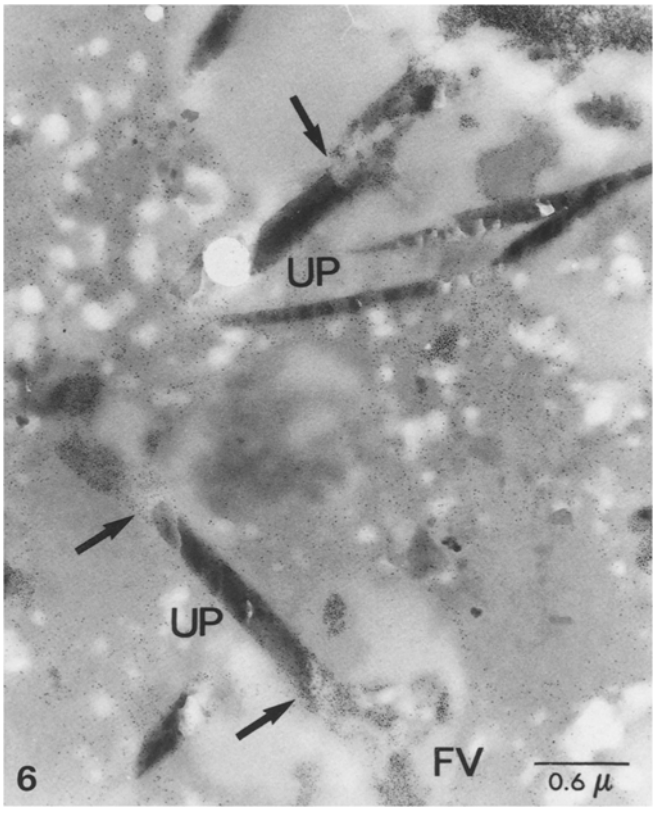

Fig. 6. Electron micrograph of a mouse hepatic parenchymal cell, 18 weeks after treatment with hexachlorobenzene plus iron dextran. Note close association between uroporphyrin crystal (*UP*) and ferritin (*arrows*). *FV* Ferritin-containing vacuole. Electron-spectroscopic image (ESI) of unstained section. *Bar*: 0.6 μm

mice treated with HCB plus IMF or with IMF alone. Up to 20 weeks, there was a steep increase in the area fractions of ferritin (HCB plus IMF: $Y=0.13X+0.07$; IMF: $Y=0.13X+0.05$). Thereafter, area fractions of ferritin gradually decreased in both treatment groups.

In the course of time, area fractions of uroporphyrin crystals gradually increased in both treatment groups. Up to 30 weeks, area fractions of uroporphyrin crystals were significantly different between mice treated with HCB plus IMF and IMF alone. At weeks 40 and 52, however, area fractions of uroporphyrin crystals were not different between the two treatment groups.

In Fig. 9 the mean ratios between the area fractions of uroporphyrin crystals and area fractions of ferritin particles at different time intervals are presented: this has been called the 'porphyrins per ferritin area fraction ratio'. As can be seen from this figure, from 2 weeks up to 20 weeks in hepatocytes of mice treated with HCB plus IMF, these ratios were relatively constant, i.e., between 0.2 and 0.3. In contrast, by the 9th week in hepatocytes of mice treated with IMF alone, the porphyrins per ferritin area fraction ratios became positive at a lower level and increased in the course of time. By the 20th week, there was a similar and sustained increase in both treatment groups in the porphyrins per ferritin area fraction ratios in the course of time (HCB plus IMF: $Y=0.004X+0.208$; IMF: $Y=0.004X+0.118$).

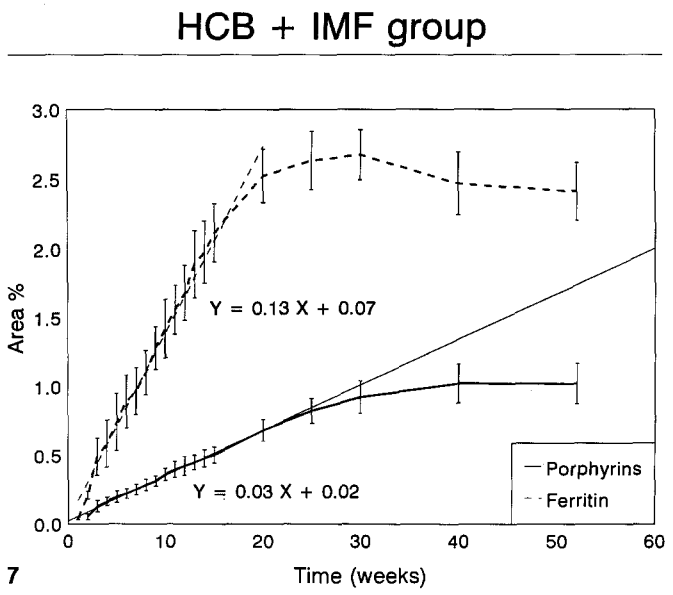

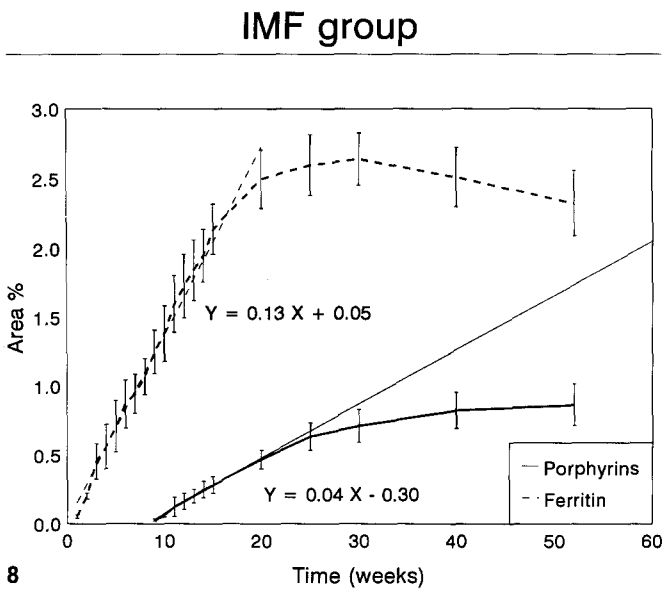

Fig. 7. Morphometrical analysis by reflection-contrast microscopy of unstained Epon sections showing area fractions of uroporphyrin crystals (*Porphyrins*) and of ferritin particles (*Ferritin*) at different time intervals in livers of mice treated with hexachlorobenzene plus iron dextran (*HCB + IMF group*). For the period up to 20 weeks, the calculated regression lines of the area fraction increase for uroporphyrin crystals and for ferritin particles are indicated

Fig. 8. Morphometrical analysis by reflection-contrast microscopy of unstained Epon sections showing area fractions of uroporphyrin crystals (*Porphyrins*) and of ferritin particles (*Ferritin*) at different time intervals in livers of mice treated with iron dextran alone (*IMF group*). For the period up to 20 weeks, the calculated regression lines of the area fraction increase for uroporphyrin crystals and for ferritin particles are indicated

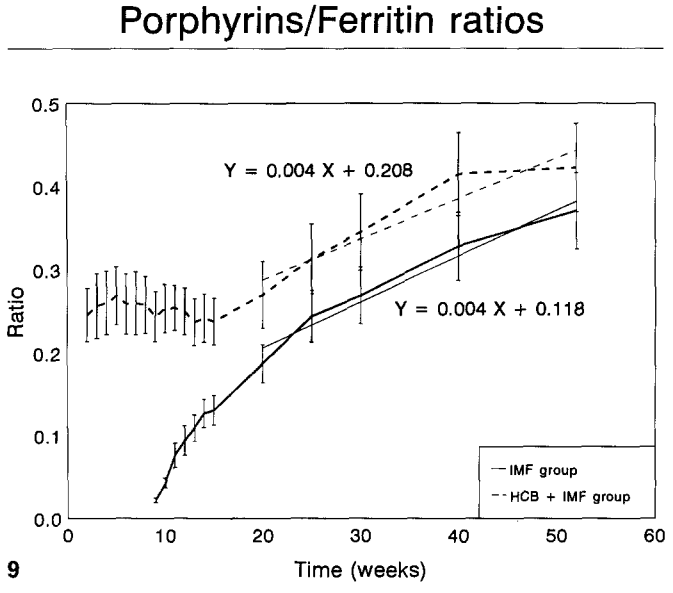

Fig. 9. Morphometrical analysis by reflection-contrast microscopy of unstained Epon sections showing ratios of porphyrins per ferritin area fractions at different time intervals in livers of mice after treatment with iron dextran (*IMF group*) and after treatment with hexachlorobenzene plus iron dextran (*HCB + IMF group*). For the period from 20 weeks up to 52 weeks, the calculated regression lines of the ratio of porphyrins per ferritin area fractions in both treatment groups are indicated

In comparing the ratios between the morphometrically determined amount of uroporphyrin crystals and of ferritin particles with the ratios between the biochemically determined porphyrin content and the iron content in livers, an identical pattern was observed in the two treatment groups (results not shown).

Discussion

In accordance with earlier findings, we confirmed that the intraperitoneal administration of HCB plus IMF, but also of IMF alone to C57BL/10 mice resulted in a time-dependent accumulation of uroporphyrin crystals in the liver. In addition, we have previously found that HCB alone, without concomitant IMF administration, does not produce (uro)porphyria in this strain of mice (Siersema et al. 1991). In the course of time, uroporphyrin crystals gradually increased in size in both treatment groups (Figs. 5, 6). We have found that in areas where uroporphyrin crystals are present, fluorescence of surrounding intracytoplasmic porphyrins can be observed as well (Siersema et al. 1991). Therefore, it seems likely that the enlargement of uroporphyrin crystals in the course of time is caused by the synthesis and apposition from surrounding porphyrins.

Our data on iron distribution in liver after administration of IMF are in agreement with observations by others, in that iron-positive staining initially was detected in Kupffer cells and siderophages, followed by the presence of ferric iron in hepatocytes in both treatment groups (Fig. 2) (Goldberg et al. 1957; Dunn 1967; Pechet 1969; Van Wyk et al. 1971; Hultcranz and Arborgh 1978; Parmley et al. 1981; Smith et al. 1990). The main storage form of iron in both treatment groups was ferritin. Morphometrically, no difference in the amount

of ferritin was observed between hepatocytes of mice treated with HCB plus IMF and with IMF alone (Figs. 7, 8). In addition, at the ultrastructural level, the distribution pattern of ferritin was not different between the two treatment groups. Therefore, it can be concluded that HCB by itself did not influence the iron accumulation into the liver.

The formation of uroporphyrin crystals developed more rapidly in livers of mice treated with HCB plus IMF than in mice treated with IMF alone, suggesting an active role for HCB in the process of uroporphyrin formation. Moreover, the morphometrical analysis revealed that for the formation of uroporphyrin crystals in hepatocytes of mice treated with IMF alone (as compared with mice treated with HCB plus IMF) much more iron (ferritin) needed to be accumulated before uroporphyrin crystal formation was initiated (Fig. 9).

HCB has been demonstrated to induce a particular isoenzyme of the cytochrome P-450 complex in the liver, cytochrome P-450la2, leading to the uncoupling of the microsomal system in the liver (Jacobs et al. 1989). Subsequently, reactive oxygen species are formed (Ferioli et al. 1984; Sweeney et al. 1984; Smith and Francis 1987; Sinclair et al. 1987; De Matteis et al. 1988). If "free" iron is present, either the highly reactive hydroxyl radical (OH·) (Aust and Svingen 1982; Halliwel and Gutteridge 1985) and/or reactive iron-oxygen species (Samokyszyn et al. 1988) are produced, which could react with uroporphyrinogen or another susceptible target to form an URO-D inhibitor (Rios de Molina et al. 1980; Cantoni et al. 1984; Smith and Francis 1987). This explains the accumulation of uroprophyrin crystals in hepatocytes (Smith et al. 1990). Alternatively, damage to URO-D either by a direct action of iron or by a free radical-mediated mechanism has been postulated (Mukerji et al. 1984). Since uroporphyria also developed in mice treated with IMF alone, induction of the cytochrome P-450 system by HCB is not an absolute requirement. Smith et al. (1990) have suggested that in hepatocytes of C57BL/10 mice a genetically determined active oxidative metabolism is present, which could explain that, after administration of IMF alone, uroporphyria develops at a slower rate (Figs. 7, 8).

A common denominator in all these theories is the presence of ferrous iron in hepatocytes. Intracellular ferrous iron, however, is mainly sequestered in ferritin in hepatocytes of C57BL/10 mice (Siersema et al. 1991) and is as such not likely to induce OH·production. The release of iron from ferritin requires reduction (Munro and Linder 1978). Although in vitro release of ferrous iron from ferritin by liver microsomes has been described (Rowley and Sweeney 1984; Samokyszyn et al. 1988; De Matteis et al. 1988), it is not clear whether this also occurs in vivo. It has been suggested that a small fraction of intracellular iron is bound to a variety of molecules of low molecular weight (LMW) (Jacobs 1977). This pool of LMW iron is thought to be more readily available for a catalytic role in the Haber-Weiss cycle. Moreover, a role for LMW iron has been demonstrated in the process of free radical formation in iron-loaded cells (Voogd et al. 1992). Therefore, a study is now in progress, using a recently developed technique (Voogd et al. 1992), to measure the amount of LMW iron in tissue homogenates to further elucidate this problem.

Acknowledgements. The authors wish to thank Dr. R.P. van Helvoirt, Mrs. A. Edixhoven-Bosdijk, Mrs. G.A.M. van Trommelen-Ketelaars, Miss C.W.J. Sorber and Mr. J. Bonnier for expert technical assistance and Mr. F.L. van der Panne for excellent photographic work.

References

Alleman MA, Koster JF, Wilson JHP, Edixhoven-Bosdijk A, Slee RG, Kroos MJ, Eijk HG van (1985) The involvement of iron and lipid peroxidation in the pathogenesis of HCB induced porphyria. Biochem Pharmacol 34:161–166

Aust SD, Svingen BA (1982) The role of iron in enzymatic lipid peroxidation. In: Pryor WA (ed) Free Radicals in Biology, vol 5. Academic Press, New York, pp 1–28

Cantoni L, Dal Fiume D, Rizzardini M, Ruggieri R (1984) In vitro inhibitory effect on porphyrinogen carboxylyase of liver extracts from TCDD treated mice. Toxicol Lett 20:211–217

Cleton MI, Mostert LJ, Sorber LWJ, Jong AAW de, Jeu-Jaspars CMH de, Bruijn WC de (1989) Effect of phlebotomy on the ferritin iron content in the rat liver as determined morphometrically with the use of electron energy loss spectroscopy. Cell Tissue Res 256:601–605

Cornelese-ten Velde I, Prins FA (1990) New sensitive light microscopical detection of colloidal gold on ultrathin sections by RCM. Combination of reflection contrast and electron microscopy in post-embedding immunogold histochemistry. Histochemistry 94:61–71

De Matteis F (1988) Role of iron in the hydrogen peroxide-dependent oxidation of hexahydroporphyrins (porphyrinogens): a possible mechanism for the exacerbation by iron of hepatic uroporphyria. Mol Pharmacol 33:463–469

De Matteis F, Harvey C, Reed C, Hempenius R (1988) Increased oxidation of uroporphyrinogen by an inducible liver microsomal system. Biochem J 250:161–169

Dunn WL (1967) Iron-loading, fibrosis and hepatic carcinogenesis. Arch Pathol 83:258–266

Ferioli A, Harvey C, De Matteis F (1984) Drug-induced accumulation of uroporphyrin in chicken hepatocyte cultures. Structural requirements for the effect and role of exogeneous iron. Biochem J 224:769–777

Goldberg L, Smith JP, Martin LE (1957) The effects of intensive and prolonged administration of iron parenterally in animals. Br J Exp Pathol 38:297–311

Halliwel B, Gutteridge JMC (1985) The importance of free radicals and catalytic metal ions in human diseases. Mol Aspects Med 8:89–193

Harris DC (1978) Iron exchange between ferritin and transferrin in vitro. Biochemistry 17:3071–3078

Hultcrantz R, Arborgh B (1978) Studies on the rat liver following iron overload. 1. Fine structural appearance. Acta Pathol Microbiol Scand Sect A 86:143–155

Jacobs A (1977) Low molecular weight intracellular iron transport compounds. Blood 50:433–439

Jacobs JM, Sinclair PR, Bement WJ, Lambrecht RW, Sinclair JF, Goldstein JA (1989) Oxidation of uroporphyrinogen by methylcholantrene-induced cytochrome P-450. Essential role of cytochrome P-450d. Biochem J 258:247–253

James KR, Cortés JM, Paradinas FJ (1980) Demonstration of intracytoplasmic needle-like inclusions in hepatocytes of patients with porphyria cutane tarda. J Clin Pathol 33:899–900

Lillie RD, Fullmer HM (1976) Histopathologic technic and practical histochemistry, 4th edn. McGraw-Hill, New York, pp 235–238, 507–508

Lowry OH, Rosebrough NJ, Farr AL, Randall RJ (1951) Protein measurement with the Folin-phenol reagent. J Biol Chem 193:265–275

Marks GS (1985) Exposure to toxic agents: the heme biosynthetic pathway and hemoproteins as indicator. CRC Crit Rev Toxicol 15:151–179

Mukerji SK, Pimstone NR, Burns M (1984) Dual mechanism of inhibition of rat liver uroporphyrinogen decarboxylase activity by ferrous iron: its potential role in the genesis of porphyria cutanea tarda. Gastroenterology 87:1248–1254

Munro HN, Linder MC (1978) Cells sequence Fe^{2+} in ferrules. Physiol Rev 58:317–396

Parmley RT, May ME, Spicer SS, Buse MG, Alvarez CJ (1981) Ultrastructural distribution of inorganic iron in normal and iron-loaded hepatic cells. Lab Invest 44:475–485

Pechet GS (1969) Parenteral iron overload: Organ and cell distribution in rats. Lab Invest 20:119–126

Ploem JS (1975) Reflection contrast microscopy as a tool for investigation of the attachment of living cells to a glass surface. In: Furth R van (ed) Mononuclear phagocytes in immunity, infection and pathology. Blackwell, Oxford, pp 405–421

Rios de Molina MDC, Wainstock de Calmanovici R, San Martin de Viale LC (1980) Investigations on the presence of porphyrinogen carboxylyase inhibitor in the liver of rats intoxicated with hexachlorobenzene. Int J Biochem 12:1027–1032

Rowley B, Sweeney GD (1984) Release of ferrous iron from ferritin by liver microsomes: a possible role in the toxicity of 2,3,7,8-tetrachlorodibenzo-p-dioxin. Can J Biochem Cell Biol 62:1293–1300

Samokyszyn VM, Thomas CE, Reif DW, Saito M, Aust SD (1988) Release of iron from ferritin and its role in oxygen radical toxicities. Drug Metab Rev 19:283–303

Scheuer PJ, Williams R, Muir AR (1962) Hepatic pathology in relatives of patients with haemochromatosis. J Pathol Bacteriol 84:53–64

Siersema PD, Helvoirt RP van, Ketelaars DAM, Cleton MI, Bruijn WC de, Wilson JHP, Eijk HG van (1991) Iron and uroporphyrin in hepatocytes of inbred mice in experimental porphyria: a biochemical and morphological study. Hepatology 14:1179–1188

Sinclair P, Lambrecht R, Sinclair J (1987) Evidence for cytochrome P450-mediated oxidation of uroporphyrinogen by cell-free liver extracts from chick embryos treated with 3-methylcholantrene. Biochem Biophys Res Commun 146:1324–1329

Smith AG, De Matteis F (1990) Oxidative injury mediated by the hepatic cytochrome P-450 system in conjunction with cellular iron. Effects on the pathway of haem biosynthesis. Xenobiotica 20:865–877

Smith AG, Francis JE (1983) Synergism of iron and hexachlorobenzene inhibits hepatic uroporphyrinogen decarboxylase in inbred mice. Biochem J 214:909–913

Smith AG, Francis JE (1987) Chemically-induced formation of an inhibitor of hepatic uroporphyrinogen decarboxylase in inbred mice with iron overload. Biochem J 246:221–226

Smith AG, Carthew P, Francis JE, Edwards RE, Dinsdale D (1990) Characterization and accumulation of ferritin in hepatocytes nuclei of mice with iron overload. Hepatology 12:1399–1405

Sorber CWJ, Jong AAW de, Breejen NJ den, Bruijn WC de (1990a) Quantitative energy-filtered image analysis in cytochemistry I. Morphometric analysis of contrast-related images. Ultramicroscopy 32:55–68

Sorber CWJ, Dort JB van, Ringeling PC, Cleton-Soeteman MI, Bruijn WC de (1990b) Quantitative energy-filtered image analysis in cytochemistry II. Morphometric analysis of element-distribution images. Ultramicroscopy 32:69–79

Sweeney GD (1986) Porphyria cutanea tarda, or the uroporphyrinogen decarboxylase deficiency diseases. Clin Biochem 19:3–15

Sweeney GD, Jones KG, Cole FM, Basford D, Krestynski F (1979) Iron deficiency prevents liver toxicity of 2,3,7,8-tetrachlorodibenzo-p-dioxin. Science 204:332–335

Sweeney GD, Basford D, Rowley B, Goddard G (1984) Mechanisms underlying the hepatotoxicity of 2,3,7,8-tetrachlorodebenzo-p-dioxin. Banbury Rep 18:225–237

Van Wyk CP, Linder-Horowitz M, Munro HN (1971) Effect of iron loading on non-heme iron compounds in different cell populations. J Biol Chem 246:1025–1031

Voogd A, Sluiter W, Eijk HG van, Koster JF (1992) Low molecular weight iron and the oxygen paradox in isolated rat hearts. J Clin Invest 90:2050–2055

Wilson JHP, Berg JWO van den, Edixhoven-Bosdijk A, Gastel-Quist LHM van den (1978) Preparation of porphyrin methylesters for high pressure liquid chromatography. Clin Chim Acta 89:165–167